NTIS#PB2024-

SSC – 480

STRENGTH OF WELDED ALUMINUM IN TENSION



Ship Structure Committee

2025

This document has been approved
for public release and sale; its
distribution is unlimited.

Documents
Document Sharing Hub

Full document details: Strength of Welded Aluminum in Tension

This page intentionally left blank

Documents
Document Sharing Hub

Full document details: Strength of Welded Aluminum in Tension

Member Agencies:

American Bureau of Shipping
Defence Research and Development Canada
Maritime Administration
Military Sealift Command
Naval Sea Systems Command
Office of Naval Research
Society of Naval Architects & Marine Engineers
Transport Canada
United States Coast Guard

Ship
Structure
Committee

Address Correspondence to:

COMMANDANT (CG-ENG-2/SSC)
ATTN (EXECUTIVE DIRECTOR/SHIP
STRUCTURE COMMITTEE)
US COAST GUARD
2703 MARTIN LUTHER KING JR. AVE SE
WASHINGTON DC 20593-7509
Website: http://www.shipstructure.org

SSC – 480
SR – 1486

STRENGTH OF WELDED ALUMINUM IN TENSION

Proper understanding of the behavior of welded aluminum components is essential for ensuring the safety and reliability of aluminum marine vessels. These vessels consist of various configurations of welded stiffened panels whose tensile behavior may not be well characterized. The change of the mechanical properties across the heat affected zone (HAZ) of the welded component should be accounted for when quantifying the ultimate strength of the member. This quantification becomes more challenging with the presence of intersecting welds or when two different alloys, each with its own HAZ properties, are welded together.

This report discusses the results of an investigation into the tensile behavior of welded aluminum components. Experimental testing was conducted to characterize the load-deformation behavior of large-scale welded aluminum specimens and their ultimate tensile capacity. The specimens covered unstiffened and stiffened plates with transverse, longitudinal, and both stiffener types. Furthermore, coupons were extracted from a butt-welded plate to quantify the change in the mechanical properties across the heat affected zone and understand how this change can impact the behavior of the large-scale specimens. Detailed three-dimensional finite element analysis was conducted and utilized to develop better understanding of the behavior of the tested specimens. The results are discussed, and recommendations are made to achieve a more accurate prediction of the tensile capacity of these specimens.

We thank the authors and Project Technical Committee for their dedication and research toward completing the objectives and tasks detailed throughout this paper and continuing the Ship Structure Committee's mission to enhance the safety of life at sea.

W. R. ARGUIN
Rear Admiral, U.S. Coast Guard
Co-Chairman, Ship Structure Committee

P. D. SMALL
Rear Admiral, U.S. Navy
Co-Chairman, Ship Structure Committee

Documents
Document Sharing Hub

Full document details: Strength of Welded Aluminum in Tension

SHIP STRUCTURE COMMITTEE

RDML Wayne Arguin
U. S. Coast Guard Assistant Commandant
for Prevention Policy (CG-5P)
Co-Chair, Ship Structure Committee

RDML Peter Small
Chief Engineer and Deputy Commander
for Naval Systems Engineering (SEA05)
Co-Chair, Ship Structure Committee

Mr. Jeffrey Lantz
Director, Commercial Regulations and Standards (CG-5PS)
U.S. Coast Guard

Mr. Gareth Burton
Vice President, Technology
American Bureau of Shipping

Mr. H. Paul Cojeen
Society of Naval Architects and Marine Engineers

Dr. Malcolm Smith
Head, Warship Performance, DGSTCO
Defense Research & Development Canada - Atlantic

Mr. Kevin Kohlmann
Director, Office of Safety
Maritime Administration

Mr. Luc Tremblay
Executive Director, Domestic Vessel Regulatory Oversight
and Boating Safety, Transport Canada

Mr. Michael Haycock
Deputy Assistant Commandant for Engineering and
Logistics (CG-4D)
U.S. Coast Guard

Mr. Mark Lattner
Group Director, Ship Integrity and Performance Engineering
(SEA 05P)
Naval Sea Systems Command

Mr. Neil Lichtenstein
Deputy Director N7x, Engineering Directorate
Military Sealift Command

Dr. Thomas Fu
Director, Ship Systems and Engineering Research Division
Office of Naval Research

SHIP STRUCTURE EXECUTIVE GROUP & SUB-COMMITTEE

UNITED STATES COAST GUARD (CVE)
CAPT Jennifer Doherty
Mr. Charles Rawson

AMERICAN BUREAU OF SHIPPING
Dr. Qing Yu
Mr. Daniel LaMere
Ms. Christina Wang
Mr. Rich Delpizzo

SOCIETY OF NAVAL ARCHITECTS AND MARINE ENGINEERS
Mr. Frederick Ashcroft
Dr. Roger Basu
Dr. Robert Sielski
Dr. Paul Miller

DEFENSE RESEARCH & DEVELOPMENT CANADA ATLANTIC
Dr. Mahmud Sazidy
Mr. Cameron Munro

MARITIME ADMINISTRATION
Mr. Todd Hiller
Mr. Todd Ripley
Mr. Digvijay Singh

TRANSPORT CANADA
Ms. Dorianne Aubin
Mr. Bashir Ahmed Golam
Ms. Tayyebe Seif

UNITED STATES COAST GUARD (FLEET)
CAPT Doug Graul
Mr. Martin Hecker
Mr. Timothy McAllister
Mr. Debu Ghosh

NAVSEA/ NSWCCD
Mr. David Qualley
Mr. Dean Schleicher
Dr. Pradeep Sensharma
Mr. Michael McDonald

MILITARY SEALIFT COMMAND
Ms. Jeannette Viernes

OFFICE OF NAVAL RESEARCH
Dr. Jessica Dibelka

Documents
Document Sharing Hub
Full document details: Strength of Welded Aluminum in Tension

PROJECT TECHNICAL COMMITTEE MEMBERS

The Ship Structure Committee greatly appreciates the contributions of the individuals that volunteered their time to participate on the Project Technical Committee, listed below, and thanks them heartily. They were the subject matter expert representatives of the Ship Structure Committee to the contractor, performing technical oversight during contracting, advising the contractor in cognizant matters pertaining to the contract of which the agencies were aware, and performing technical peer review of the work in progress and upon completion.

Chair:
Mr. Charles Rawson, U.S. Coast Guard

Members:
Dr. Robert Sielski, Society of Naval Architecture and Marine Engineers
Dr. Jonah Klemm-Toole, Colorado School of Mines
Dr. Zhenzhen Yu, Colorado School of Mines
Dr. Paul Hess, StructRel Solutions
Mr. Debu Ghosh, U.S. Coast Guard
Mr. Spencer Johnson, Austal
Dr. Libin Miao, American Bureau of Shipping
Mr. Ajoy Kumar, BMT Designers & Planners
Ms. Jeannette Viernes, Military Sealift Command
Dr. Igor Chavez, University of Newcastle
Mr. Rod Sutherland, NDI Engineering

Ship Structure Committee Executive Director:
LCDR Bryan Andrews, U.S. Coast Guard

Documents
Document Sharing Hub
Full document details: Strength of Welded Aluminum in Tension

Technical Report Documentation Page

1. Report No. SSC-480	2. Government Accession No.	3. Recipient's Catalog No.
4. Title and Subtitle Strength of Welded Aluminum in Tension		5. Report Date 3 June 2025
		6. Performing Organization Code
7. Author(s) Dr. Mohamed Soliman, Ph.D Alaaeldin T. Soliman		8. Performing Organization Report No. SR-1486
9.Performing Organization Name and Address School of Civil & Environmental Engineering, Oklahoma State University 222 Engineering North, Stillwater, OK 74078		10. Work Unit No. (TRAIS)
		11. Contract or Grant No.
12. Sponsoring Agency Name and Address Ship Structure Committee C/O US Coast Guard 2703 Martin Luther King Jr. Ave. SE Washington, DC 20593-7509		13. Type of Report and Period Covered Final Report
		14. Sponsoring Agency Code CG-5PS
15. Supplementary Notes		

16. Abstract

This report discusses the results of an investigation into the tensile behavior of welded aluminum components. Experimental testing was conducted to characterize the load-deformation behavior of large-scale welded aluminum specimens and their ultimate tensile capacity. The specimens covered unstiffened and stiffened plates with transverse, longitudinal, and both stiffener types. Furthermore, coupons were extracted from a butt-welded plate to quantify the change in the mechanical properties across the heat affected zone and understand how this change can impact the behavior of the large-scale specimens. Detailed three-dimensional finite element analysis was conducted and utilized to develop better understanding of the behavior of the tested specimens. The results are discussed, and recommendations are made to achieve a more accurate prediction of the tensile capacity of these specimens.

17. Key Words Weld repair, aluminum, low-heat input		18. Distribution Statement Approved for public release; distribution is unlimited. Available from: National Technical Information Service Springfield, VA 22161 (703) 487-465	
19. Security Classif. (of this report) Unclassified	20. Security Classif. (of this page) Unclassified	21. No. of Pages 133	22. Price

Documents
Document Sharing Hub
Full document details: Strength of Welded Aluminum in Tension

Conversion Factors
(Approximate conversion to metric measures)

To convert from	to	Function	Value
LENGTH			
inches	meters	divide	39.3701
inches	millimeters	multiply by	25.4000
feet	meters	divide by	3.2808
VOLUME			
cubic feet	cubic meters	divide by	35.3149
cubic inches	cubic meters	divide by	61,024
SECTION MODULUS			
$inches^2$ feet	$centimeters^2$ meters	multiply by	1.9665
$inches^2$ feet	$centimeters^3$	multiply by	196.6448
$inches^3$	$centimeters^3$	multiply by	16.3871
MOMENT OF INERTIA			
$inches^2$ $feet^2$	$centimeters^2$ $meters^2$	divide by	1.6684
$inches^2$ $feet^2$	$centimeters^4$	multiply by	5993.73
$inches^4$	$centimeters^4$	multiply by	41.623
FORCE OR MASS			
long tons	tonnes	multiply by	1.0160
long tons	kilograms	multiply by	1016.047
pounds	tonnes	divide by	2204.62
pounds	kilograms	divide by	2.2046
pounds	Newtons	multiply by	4.4482
PRESSURE OR STRESS			
$pounds/inch^2$	$Newtons/meter^2$ (Pascals)	multiply by	6894.757
kilo $pounds/inch^2$	mega $Newtons/meter^2$ (mega Pascals)	multiply by	6.8947
BENDING OR TORQUE			
foot tons	meter tons	divide by	3.2291
foot pounds	kilogram meters	divide by	7.23285
foot pounds	Newton meters	multiply by	1.35582
ENERGY			
foot pounds	Joules	multiply by	1.355826
STRESS INTENSITY			
kilo $pound/inch^2$ $inch^{½}$ ($ksi\sqrt{in}$)	mega Newton $MNm^{3/2}$	multiply by	1.0998
J-INTEGRAL			
kilo pound/inch	$Joules/mm^2$	multiply by	0.1753
kilo pound/inch	kilo $Joules/m^2$	multiply by	175.3

Documents
Document Sharing Hub
Full document details: Strength of Welded Aluminum in Tension

STRENGTH OF WELDED ALUMINUM IN TENSION

Prepared by

Dr. Mohamed Soliman, Ph.D., Associate Professor
School of Civil & Environmental Engineering, Oklahoma State University
222 Engineering North, Stillwater, OK 74078,
Phone: 405-744-9777, Email: mohamed.soliman@okstate.edu,
Website: http://www.mohamedsoliman.info

Alaaeldin T. Soliman, Former M.Sc. Student,
School of Civil & Environmental Engineering, Oklahoma State University

Submitted to

Ship Structure Committee

March 2024

Documents
Document Sharing Hub

Full document details: Strength of Welded Aluminum in Tension

ABSTRACT

This report discusses the results of an investigation into the tensile behavior of welded aluminum components. Experimental testing was conducted to characterize the load-deformation behavior of large-scale welded aluminum specimens and their ultimate tensile capacity. The specimens covered unstiffened and stiffened plates with transverse, longitudinal, and both stiffener types. Furthermore, coupons were extracted from a butt-welded plate to quantify the change in the mechanical properties across the heat affected zone and understand how this change can impact the behavior of the large-scale specimens. Detailed three-dimensional finite element analysis was conducted and utilized to develop better understanding of the behavior of the tested specimens. The results are discussed, and recommendations are made to achieve a more accurate prediction of the tensile capacity of these specimens.

Documents
Document Sharing Hub

Full document details: Strength of Welded Aluminum in Tension

EXECUTIVE SUMMARY

Proper understanding of the behavior of welded aluminum components is essential for ensuring the safety and reliability of aluminum marine vessels. These vessels consist of various configurations of welded stiffened panels whose tensile behavior may not be well characterized. The change of the mechanical properties across the heat affected zone (HAZ) of the welded component should be accounted for when quantifying the ultimate strength of the member. This quantification becomes more challenging with the presence of intersecting welds or when two different alloys, each with its own HAZ properties, are welded together.

The tensile behavior of these complex configurations has not been experimentally investigated in literature, especially on a larger scale closer to that adopted in ships. Therefore, a comprehensive testing program, covering AA5083-H116 and AA6061-T6511 alloys, was conducted to characterize the tensile behavior of welded components made of both alloys. Baseline information on the mechanical properties of the utilized alloys, and their HAZ, was established through small-scale coupon testing. Next, large-scale testing was conducted on specimens consisting of flat plates, in addition to plates with transversely welded stiffeners, longitudinally welded stiffeners, and with both stiffener types. In total, twelve large-scale specimens were tested with three replicas for each specimen type to shed some light on the uncertainty of the behavior. Numerical finite element analysis was conducted to develop a better understanding of the behavior of these welded specimens and identify the underlying parameters that govern the response. Available strength prediction models are evaluated and compared to the experimental results.

The experimental results showed the expected increase in strength that accompanies the addition of longitudinal stiffeners; however, the inclusion of transversally welded stiffener did not have a significant impact on the capacity of the AA5083 specimens. The experimental results, however, highlighted the drop in ductility that occurs for the specimens with both stiffener types. The conducted testing and analysis also showed that available strength prediction models may not provide consistent safety factors for different specimen types and highlighted the importance of considering strain compatibility when quantifying the ultimate tensile strength of some of these specimens.

Documents
Document Sharing Hub
Full document details: Strength of Welded Aluminum in Tension

ACKNOWLEDGMENTS

The authors gratefully acknowledge the financial support from the United States Coast Guard (USCG), Award number SR-1486. The authors would like to thank Mr. Charles Rawson, Naval Architecture Division of the USCG, and the Project Technical Committee for their guidance and help throughout the duration of the project. The contribution of AUSTAL, USA, in the form of donating the fabricated specimens that were essential for completing this research, is greatly acknowledged. Special thanks to Mr. Spencer Johnson and Mr. Shawn Wilber from AUSTAL, USA for their help during the design and fabrication phases of the project. The authors would also like to acknowledge W&W|AFCO STEEL for donating the fabricated steel grip assemblies. Finally, we would like to thank the team of graduate, undergraduate, and high school research assistants at Oklahoma State University who helped with the experimental program. This team included Cody James, Aditya Nayak, Seth Prizznick, Jacob Schindall, Cooper Waddell, Jaxson Spears, Della Thomas, Hunter Moulayiansis, Ahmad Shanawaz, Carter Israelson, Joshua Exline, Yassin Soliman, Jocelynn Swann, Diego Valencia, and Mr. David Porter, the lab supervisor for Bert Cooper Engineering Laboratory at Oklahoma State University.

Documents
Document Sharing Hub

Full document details: Strength of Welded Aluminum in Tension

TABLE OF CONTENTS

Section Page

1 INTRODUCTION 1
2 LITERATURE REVIEW 4
2.1 MECHANICAL PROPERTIES ACROSS THE HAZ 4
2.2 RESIDUAL STRESSES AND THEIR DISTRIBUTION IN WELDED ALUMINUM JOINTS 7
2.3 VARIABILITY IN THE MECHANICAL PROPERTIES OF ALUMINUM ALLOYS 12
2.4 TENSILE STRENGTH PREDICTION OF WELDED ALUMINUM PANELS 16
2.4.1 Aluminum Design Methods 16
2.4.2 FE modelling for predicting the tensile strength of welded aluminum panels 17
3 EXPERIMENTAL TESTING PROGRAM 22
3.1 ANCILLARY TESTING 22
3.2 LARGE SCALE EXPERIMENTAL SETUP 24
3.2.1 Original Test Setup 24
3.2.1.1 Upper and Lower Steel Grip Assemblies 26
3.2.2 Updated Test Setup 28
3.2.3 Hydraulic System and Test Control 35
3.2.4 Test Matrix for the Large-Scale Testing Program 37
3.3 ALUMINUM SPECIMEN DESIGN 37
3.3.1 Flat Plate Specimens 40
3.3.2 Transverse Stiffener Specimens 41
3.3.3 Longitudinal Stiffener Specimens 43
3.3.4 Longitudinal and Transverse Stiffener Specimens 44
3.3.5 Connection between Steel End Plate and Aluminum End Plate 45
3.4 INSTRUMENTATION 46
3.5 TEST PROCEDURE 49
3.5.1 Ancillary Testing 49
3.5.2 Large-Scale Testing 50
3.6 TESTING OF THE INITIAL ALUMINUM SPECIMEN 51
4 EXPERIMENTAL RESULTS 54
4.1 ANCILLARY TESTING 54

Documents
Document Sharing Hub
Full document details: Strength of Welded Aluminum in Tension

4.2 LARGE-SCALE TESTING....61
4.2.1 Testing Results....61
4.2.1.1 Flat Plate Specimen Results....61
4.2.1.2 Transverse Stiffener Specimen Results....70
4.2.1.3 Longitudinal Stiffener Specimen Results....78
4.2.1.4 Longitudinal and Transverse Stiffener Specimen Results....86
5 FINITE ELEMENT MODELLING....95
5.1 MODEL GEOMETRY....95
5.2 MATERIAL MODELING....97
5.2.1 Aluminum Stress-Strain Behavior....97
5.2.2 Ductile Damage Model....99
5.3 OTHER MODEL ATTRIBUTES....100
5.4 FINITE ELEMENT MODELLING RESULTS....105
6 DISCUSSION....113
6.1 EFFECT OF SPECIMEN SIZE ON STRENGTH AND DUCTILITY....113
6.2 EFFECT OF WELDING ON THE BEHAVIOR OF WELDED ALUMINUM COMPONENTS....115
6.3 ULTIMATE STRENGTH PREDICTION....117
6.4 SIMPLIFICATIONS TO THE FINITE ELEMENT MODELING PROCEDURE....121
6.4.1 Effect of the residual stresses....122
6.4.2 Effect of modeling the weld lines....123
6.4.3 Simplified mechanical properties of the HAZ....125
7 CONCLUSIONS AND RECOMMENDATIONS FOR FUTURE WORK....128
7.1 CONCLUSIONS....128
7.2 RECOMMENDATIONS FOR FUTURE WORK....129
8 REFERENCES....131

Documents
Document Sharing Hub
Full document details: Strength of Welded Aluminum in Tension

LIST OF TABLES

Table Page

Table 2.1: Magnitude and distribution of residual stresses in AA5083-H116 reported in literature 10

Table 2.2: Magnitude and distribution of residual stresses in AA6061-T6 reported in literature 11

Table 2.3: Mechanical properties of AA5083-H116. 15

Table 2.4: Mechanical properties of AA6061-T6. 15

Table 3.1: Test matrix for the large-scale testing program 37

Table 3.2: Mechanical properties of AA5083-H116 utilized in specimen design. 39

Table 3.3: Mechanical properties of AA6061-T6 utilized in specimen design. 39

Table 4.1: Stress-strain characteristics of AA5083-H116 HAZ coupons 57

Table 4.2: Stress-strain characteristics of AA6061-T6511 HAZ coupons 57

Table 4.3: Stress-strain characteristics of 5183 weld metal coupons 58

Table 4.4: Strength characteristics of AA5083-H116 BM Coupons 60

Table 4.5: Strength characteristics of AA6061-T6511 BM Coupons 60

Table 4.6: Results of flat plate specimens 61

Table 4.7: Results of Transverse Stiffener Specimens 71

Table 4.8: Results of Longitudinal Stiffener Specimens 79

Table 4.9: Results of Longitudinal and Transverse Stiffener Specimens 91

Table 5.1: Modified Ramberg-Osgood model parameters. 99

Table 6.1: Comparison of the specimen capacity obtained from the experimental results, FE modeling, and the *Aluminum Design Manual* (AA 2020). 118

Table 6.2: Comparison of the ultimate elongation between the experimental results and FEM. 121

Documents
Document Sharing Hub

Full document details: Strength of Welded Aluminum in Tension

LIST OF FIGURES

Figure Page

Figure 2.1: Typical hardness profile of butt welded joint (adapted from Pérez et al. (2016)). 5

Figure 2.2: Illustrative figure showing the residual stress distribution from butt welds (a) deposition of butt weld, (b) contraction of butt weld, (c) restraint forces between BM and weld, (d) formation of longitudinal residual stresses, and (e) formation of transverse residual stresses (Gurney, 1979). 9

Figure 2.3: Stress-Strain curves for the HAZ of AA6061-T6 (adapted from Nazemi and Ghrib (2019)) 20

Figure 3.1: Dimensions of welded specimen for coupon testing in millimeters. 23

Figure 3.2: Dimensions of coupons that are to be cut using a waterjet in millimeters. 24

Figure 3.3: The 1,500 KN Universal Testing Machine. 25

Figure 3.4: 3D render of the original test setup showing various specimen components. 25

Figure 3.5: Original test setup with assembly in place. 26

Figure 3.6: 3D render for the Steel Grip Assembly. 27

Figure 3.7: Detailed dimensions of the Steel Grip Assembly in millimeters. 28

Figure 3.8: General layout of the updated test setup. 29

Figure 3.9: 3D render of the updated test setup showing various specimen components. 29

Figure 3.10: Overall dimensions of the updated test setup in millimeters. 30

Figure 3.11: Detailed layout of the modified steel grip assemblies (a) dimensions of the modified upper and lower steel grip plates in millimeters, and (b) 3D render of the modified upper steel grip plate. 30

Figure 3.12: Loading Beam (W16×89) with upper pin connection and the spacer. 31

Figure 3.13: Various components of Load Column 1. 32

Figure 3.14: Various components of Load Column 2. 32

Figure 3.15: Connection to the strong floor. 33

Figure 3.16: View of the lateral support system attached to the loading beam. 34

Figure 3.17: Closeup view on the roller bearing that accommodates the in-plane movement. 34

Figure 3.18: The updated test setup. 35

Figure 3.19: Components of the hydraulic system in Load Column 1. 36

Figure 3.20: Components of the hydraulic system in Load Column 2. 36

Figure 3.21: Comparison between the steel grip assemblies: (a) original test setup and (b) updated test setup. 38

Figure 3.22: General layout of the Flat Plate Specimen. 39

Figure 3.23: Dimensions of the main test plate in millimeters. 40

Documents
Document Sharing Hub

Full document details: Strength of Welded Aluminum in Tension

Figure 3.24: Dimensions of upper and lower aluminum end plate in millimeters. 41
Figure 3.25: Dimensions of the connection stiffeners in millimeters. 41
Figure 3.26: Dimensions of the flat plate specimen (in millimeters). 42
Figure 3.27: General layout of the transverse stiffener specimen (a) dimensions (in millimeters) and (b) 3D render of the T specimen. 42
Figure 3.28: Dimensions of the longitudinal stiffener in millimeters. 43
Figure 3.29: Dimensions of the smaller connection stiffeners found in L and LT Specimens..... 43
Figure 3.30: General layout of the longitudinal stiffener specimen (a) dimensions (in millimeters) and (b) 3D render of the L specimen. 44
Figure 3.31: General layout of the longitudinal and transverse stiffener specimen (a) dimensions (in millimeters) and (b) 3D render of the LT specimen. 44
Figure 3.32: Dimensions of the steel plate washer in millimeters. 45
Figure 3.33: The utilized bolt assembly. 45
Figure 3.34: NI cDAQ-9178 with the different cards attached for recording data. 46
Figure 3.35: Location of the strain gauges for different types of specimens (a) F specimens, (b) T specimens, (c) L specimens, and (d) LT specimens. 47
Figure 3.36: Attachment of the LVDTs for different specimens (a) F specimens, (b) T specimens, (c) L specimens, and (d) LT specimens. 48
Figure 3.37: Components of the DIC system. 49
Figure 3.38: Components of the initial aluminum specimen (a) The initial aluminum specimen along with the BM and HAZ plates (b) The steel grip assembly. 51
Figure 3.39: The initial aluminum specimen during testing (a) location of the extensometer, (b) general view, and (c) location of the strain gauges. 52
Figure 3.40: Original test setup for the initial aluminum specimen. 53
Figure 3.41: Initial test specimen after failure: (a) general view and (b) close up view of the fracture surface. 53
Figure 4.1: Coupons used in ancillary testing (a) location of HAZ coupons after they were extracted from the welded specimen, (b) HAZ coupons for AA5083-H116, (c) HAZ coupons for AA6061-T6 (d) BM coupons for AA6061-T6 (e) BM coupons for AA5083-H116. 54
Figure 4.2: Close-up view for one of the AA5083-H116 HAZ coupons after the test was completed. 55
Figure 4.3: Stress-Strain curves across the HAZ for AA5083-H116. 55
Figure 4.4: Stress-Strain curves across the HAZ for AA6061-T6511. 56
Figure 4.5: Stress-Strain curves of the base metal coupons of AA5083-H116. 59
Figure 4.6: Stress-Strain curves of the base metal coupons of AA6061-T6511. 59
Figure 4.7: Load-deformation curves of flat plate specimens. 62
Figure 4.8: Flat plat specimen post failure (a) F1, (b) F2, and (c) F3. 64

Documents
Document Sharing Hub
Full document details: Strength of Welded Aluminum in Tension

Figure 4.9 Fracture surfaces of Specimen F3: (a) upper fracture surface and (b) lower fracture surface (other specimens showed similar behavior) 65

Figure 4.10: DIC results for specimen F1 (a) strain before the onset of serration, (b) strain at the onset of the first serration, and (c) strain towards the end of the test. 67

Figure 4.11: DIC results for specimen F2 (a) strain before the onset of serration, (b) strain at the onset of the first serration, and (c) strain towards the end of the test. 68

Figure 4.12: DIC results for specimen F1 (a) strain at the beginning of the test, (b) strain at the onset of the first serration, and (c) strain towards the end of the test. 69

Figure 4.13: Specimen F1 results: (a) load vs time showing the onset of serrations, and (b) strain vs time showing strain readings and how they react to the onset of serrations. 70

Figure 4.14: Load-deformation curves for all transverse stiffener specimens..... 71

Figure 4.15: Failure of the T specimens: (a) general location of failure, (b) upper fracture surface of Specimen T2, and (c) lower fracture surface of T2. 72

Figure 4.16: Transverse stiffener specimen post failure (a) T1 (b) T2 (c) T3 74

Figure 4.17: DIC results for specimen T1 (a) strain before the onset of serrations, (b) strain at the onset of the first serration, and (c) strain towards the end of the test. 75

Figure 4.18: DIC results for specimen T2 (a) strain before the onset of serrations, (b) strain at the onset of the first serration, and (c) strain towards the end of the test. 76

Figure 4.19: DIC results for specimen T3 (a) strain before the onset of serrations, (b) strain at the onset of the first serration, and (c) strain towards the end of the test. 77

Figure 4.20: Load-deformation curves for all longitudinal stiffener specimens. 78

Figure 4.21 Failure surfaces of Specimen L2 (a) lower 5083 surface, (b) lower 6061 surface, (c) upper 5083 surface, and (d) upper 6061 surface. 80

Figure 4.22: Longitudinal stiffener specimen post failure (a) L1 (b) L2 (c) L3. 82

Figure 4.23: DIC results for specimen L1 (a) strain in the beginning of the test, (b) strain just before the onset of the first serration, and (c) strain after the single serration where the specimen failed shortly after. (The shown segment is the main test plate) 83

Figure 4.24: DIC results for specimen L2 (a) strain in the beginning of the test, (b) strain just before the onset of the first serration, and (c) strain after the single serration where the specimen failed shortly after. (Left segment is the main test plate and the right segment is the stiffener) 84

Figure 4.25: DIC results for specimen L3 (a) strain in the beginning of the test, (b) strain just before the onset of the first serration, and (c) strain after the single serration where the specimen failed shortly after. (Left segment is the main test plate and the right segment is the stiffener) 85

Figure 4.26: Load-deformation curves for all LT specimens. 86

Figure 4.27 Lower failure surface of Specimen LT2 with focus are covering: (a) the AA5083 failure surface and (b) the AA8061 surface 87

Figure 4.28: Longitudinal and transverse stiffener specimen post failure (a) LT1, (b) LT2, and (c) LT3..... 89

Documents
Document Sharing Hub

Full document details: Strength of Welded Aluminum in Tension

Figure 4.29: Failure of the LT specimen (a) fracture of the longitudinal stiffener and (b) necking of the stiffener on the other side of the fracture location. 90

Figure 4.30: DIC results of specimen LT 1 (a) strain in the beginning of the test, (b) strain in the middle of the test, and (c) strain before the end of the test. (Left segment is the main test plate and the right segment is the stiffener) 92

Figure 4.31: DIC results of specimen LT 2 (a) strain in the beginning of the test, (b) strain in the middle of the test, and (c) strain before the end of the test. (Left segment is the main test plate and the right segment is the stiffener) 93

Figure 4.32: DIC results of specimen LT 3 (a) strain in the beginning of the test, (b) strain in the middle of the test, and (c) strain before the end of the test. (Left segment is the main test plate and the right segment is the stiffener) 94

Figure 5.1: Model geometry of the F specimen (a) 3D view of the FE model, (b) different components in the FE model 95

Figure 5.2: Model geometry of the T specimen (a) 3D view of the FE model, (b) different components in the FE model 96

Figure 5.3: Model geometry of the L specimen (a) 3D view of the FE model, (b) different components in the FE model 96

Figure 5.4: Model geometry of the LT specimen (a) 3D view of the FE model, (b) different components in the FE model 97

Figure 5.5: Comparison between the original and modified Ramberg-Osgood model vs the experimental profile reported in Yun et al. (2021). 98

Figure 5.6: Illustrative figure for the Ductile Damage Model. 100

Figure 5.7: Meshing of different model components: (a) mesh orientation of the main test plate, (b) mesh orientation of the longitudinal stiffener, and (c) mesh orientation of the transverse stiffener found in T specimens. 101

Figure 5.8: Tie constraint between connection stiffeners and main test plate. 101

Figure 5.9: Close-up view on the HAZ sectioning in the LT specimen FE model 102

Figure 5.10: Close-up view on the weld lines used to connect the different parts in the LT specimen FE model. 103

Figure 5.11: Boundary conditions across all FE models (a) bottom fixed support at the lower aluminum end plate, and (b) displacement applied from the upper aluminum end plate. 103

Figure 5.12: Predefined fields of residual stresses in L Specimen FE model 104

Figure 5.13: Internal and kinematic energy on one of the finite element models. 105

Figure 5.14: Finite element model results for flat plate specimens. 106

Figure 5.15: Behavior of flat plate specimen FE model (a) overall failure and (b) close-up view on the failure. 106

Figure 5.16: Finite element model results for transverse stiffener specimens. 107

Documents
Document Sharing Hub

Full document details: Strength of Welded Aluminum in Tension

Figure 5.17: Comparison between the failure location of the experimental test and FE model in T specimens (a) failure of specimen T3 and (b) close-up view on the failure in the FE model. 108

Figure 5.18: Finite element model results for longitudinal stiffener specimens..... 109

Figure 5.19: Overall failure of longitudinal stiffener specimen FE model..... 109

Figure 5.20: Behavior of longitudinal stiffener specimen FE model (a) failure of the main test plate and (b) overall failure..... 110

Figure 5.21: Finite element model results for the LT specimens. 111

Figure 5.22: Overall failure of longitudinal and transverse stiffener specimen FE model..... 111

Figure 5.23: Behavior of the FE model of LT specimens (a) failure of the stiffener prior to the overall failure, (b) overall failure, and (c) failure of specimen T3 in the same manner (note the post failure orientation of the transverse stiffener that was captured by the FE model). 112

Figure 6.1: Stress-Strain curves of large scale and small-scale base metal tests of AA5083..... 113

Figure 6.2: Different shapes of serrations of AA5083 (a) close-up view on the shape of the serrations in the small-scale coupons (b) close-up on the shape of serrations in the large-scale flat plate specimen. 115

Figure 6.3: Visual appearance of serrations (a) closely spaced serrations in the small-scale coupons, and (b) widely spaced serrations in large-scale specimens. 115

Figure 6.4: Load-deformation curves for the average of each stiffener configuration..... 117

Figure 6.5: Stress-strain profiles of different components governing the strength of the LT specimens..... 120

Figure 6.6: Load-defomration curves of Specimen T3 along with the original FE results and the FE results without residual stresses. 122

Figure 6.7: Load-defomration curves of Specimen L2 along with the original FE results and the FE results without residual stresses. 123

Figure 6.8: Load-defomration curves of Specimen T3 along with the original FE results and the FE results with no weld lines..... 124

Figure 6.9: Load-defomration curves of Specimen L2 along with the original FE results and the FE results with no weld lines..... 124

Figure 6.10: Load-defomration curves of Specimen LT3 along with the original FE results and the FE results with no weld lines..... 125

Figure 6.11: Load-deformation curves of Specimen T3, the original FE model, and FE models with different HAZ zones assigned to the full extent of the HAZ..... 126

Figure 6.12: Load-deformation curves showing the average LT specimen, the original FEM and FE models with different HAZ zones assigned to the full extent of the HAZ..... 127

Documents
Document Sharing Hub

Full document details: Strength of Welded Aluminum in Tension

1 INTRODUCTION

Aluminum alloys are widely used in marine structures due to their good formability, high strength-to-weight ratio, and lightweight characteristics. They also have high resistance to corrosion which makes them especially suitable for utilization in aggressive marine environments. Aluminum alloys used in marine structures include the 4xxx, 5xxx, and 6xxx series alloys. The 4xxx-series is an aluminum-silicon alloy used primarily in castings or as the weld filler metal for other aluminum alloys. The 5xxx-series is an aluminum-magnesium alloy with high corrosion resistance that is suitable for components in direct contact with sea water. The aluminum-magnesium-silicon 6xxx-series alloys are utilized to manufacture extruded sections with adequate corrosion resistance for marine environments. The widely used aluminum alloys in marine construction include AA5083-H116, AA6061-T6, AA6082, and AA5086. The AA5083-H116 is typically rolled and commonly utilized as the hull plate, while AA6061-T6 comes as extruded sections and is generally used for stiffeners.

Despite these appealing characteristics, the structural behavior and fabrication methods of aluminum structural components can be significantly different compared to those of traditional steel vessels. This can pose challenges associated with their use in ship building and requires more research to properly understand their behavior and develop appropriate design techniques that ensure the reliability and longevity of the vessel. A main factor that affects the behavior of aluminum alloys when utilized in ship building is the inferior mechanical properties of the weld heat affected zone (HAZ) of some alloys when compared to those of the base metal. The HAZ is the area within the structural component that is affected by the heat generated from the welding process. As a result of heating, the mechanical properties across the HAZ deteriorate due to the phase transformation of the hardening precipitates from the strong needle-like form (i.e., β") to the granular, more porous form (i.e., β). This phase transformation is caused by the high, concentrated heat input applied to this small area (Torres & Vargas, 2013). The welding process also creates residual stress fields that get locked into the material and may affect the structural behavior under subsequent loading applied during the service life. For a typical stiffened panel, the welding process creates high tensile residual stresses at the stiffener weld lines and compressive stresses in between the stiffeners (Paik et al., 2008). The high tensile residual stresses around the welds may

Documents
Document Sharing Hub
Full document details: Strength of Welded Aluminum in Tension

promote the growth of cracks in the weld zone and may affect the load bearing capacity of the panel (Lu et al., 2020).

An additional challenge associated with aluminum design is the variability in the reported mechanical properties of commonly used alloys having the same temper and heat treatment. For example, Lakshminarayanan et al. (2009), Pérez et al. (2016), and Arun and Ramachandran (2015) reported a tensile yield strength ranging from 240 MPa (34.8 ksi) to 300 MPa (43.5 ksi) for AA6061-T6. The ultimate tensile strength for the same alloy ranged from 295 MPa (42.8 ksi) to 335 MPa (48.6 ksi) in these studies. Design codes and standards, e.g., *European Committee for Standardization (EN) 485-2* (CEN, 2013) and the *Aluminum Design Manual* published by the Aluminum Association (AA 2020) typically adopt conservative values of the mechanical properties to maintain an acceptable reliability level for the designed components. For this particular alloy (i.e., AA6061-T6), the EN 485-2 (CEN 2013) and the *Aluminum Design Manual* (AA 2020) specify yield and ultimate strengths of 240 MPa (34.8 ksi) and 290 MPa (42 ksi), respectively. This level of conservatism may unnecessarily increase the initial construction cost of the ship and increase its weight leading to higher running costs throughout the service life.

This variability in the mechanical properties can be attributed to several parameters that have been shown to impact the reported values of mechanical properties. These parameters include the strain rate of loading, specimen size, and rolling direction, among others. For instance, Zhang et al. (2022) studied the effect of the strain rate on the obtained mechanical properties of AA6061-T6. Tensile tests were conducted with strain rates ranging from 0.001/s to 4732/s. The reported yield strengths varied from 220 MPa (32 ksi) to 300 MPa (43.5 ksi) with the large increase in the strength occurring past a strain rate of 984/s. A study conducted by Clausen et al. (2001) investigated the effect of specimen geometry and rolling direction on the mechanical properties of AA6082 and AA7108. Large and small coupons were extracted from different rolling directions and tested under tensile loading. Both aluminum alloys showed a change in the yield strength when the coupon size changed. In addition, the mechanical properties exhibited a decrease in strength when the rolling direction shifted from 0^o to 45^o and an increase when it changes from 45^o to 90^o. Accordingly, in addition to the inherent randomness arising from the alloying process, more uncertainty in predicting the behavior is introduced due to the fabrication process and the testing procedure used to establish the mechanical properties.

Documents
Document Sharing Hub
Full document details: Strength of Welded Aluminum in Tension

Welding is the primary fabrication method used in ship construction. For aluminum ship construction, the weld filler metal may be weaker than the base metal or its HAZ; thus, the weld strength may govern the capacity of the connection. The welds in this case are referred to as under-matched welds. The fabrication of stiffened panels with longitudinal and transverse stiffeners requires weld lines in various orientations leading to the potential of intersecting welds and/or HAZs. Quantifying the strength of the panel in these situations becomes even more challenging. A recent study by Collette (2022) investigated, experimentally and through finite element modeling (FEM), the effect of undermatched welds on the tensile strength of aluminum plates with transversally welded stiffeners. The study concluded that these types of welds could pose a possible risk to ship hull girders due to the localization of plastic deformation in the undermatched regions. However, no analysis was conducted to investigate the effect of other welding orientations, also common in ship construction, on the tensile behavior of aluminum components.

To address this need, this report investigates, both experimentally and numerically, the behavior of large-scale welded aluminum components consisting of non-load carrying fillet welds, load carrying fillet welds, and a combination of both types. In this report, load carrying fillet welds refer to those welds transferring forces in the main direction of loading of the shell plate, while non load carrying welds do not participate in the primary load transfer mechanism. AA5083-H116 (ASTM B928) and AA6061-T6511 (ASTM B221) are the aluminum alloys covered in the research. The AA5083 aluminum alloy is used as the main plate material that is stiffened by AA6061 plates. Large-scale testing is conducted on four configurations of specimens: a flat plate specimen, longitudinally stiffened specimen, transversely stiffened specimen, and a specimen that combined both stiffener types. The change in the mechanical properties across the HAZ is investigated through an experimental testing program on small-scale coupons extracted from welded specimens. Finite element (FE) analysis is also conducted in ABAQUS environment to develop better understanding of the behavior. This FE analysis included the fillet weld lines, residual stresses, and variation of the mechanical properties across the HAZ. The report first discusses available literature, then presents the details of the experimental investigation and the finite element analysis. Finally, it discusses the results and investigates possible simplifications to the finite element procedure to reduce the computational cost of the analysis.

Documents
Document Sharing Hub
Full document details: Strength of Welded Aluminum in Tension

2 LITERATURE REVIEW

The non-heat-treated (5xxx-series) and the heat-treated (6xxx-series) aluminum alloys are used widely across the marine industry. The 5xxx-series alloys are primarily composed of aluminum and magnesium, while the 6xxx-series alloys mainly consist of aluminum, magnesium, and silicon. The 5xxx-series alloys are usually produced as rolled plates and they gain their strength after being strain hardened (cold rolled) at the mill. On the other hand, 6xxx-series components are usually produced as extruded shapes. The corrosion resistance of the 5xxx-series alloys is generally better than that of the 6xxx-series alloys. As a result, 5xxx-series are typically utilized in hull plating with the 6xxx-series alloys as extruded stiffeners that are welded to the plating. This construction configuration with two different aluminum alloys welded using a different filler metal, each with its own load-deformation behavior, poses a challenge in predicting the ultimate strength of welded aluminum panels under tensile loading. The issue of strength prediction is exacerbated by the high variability in the mechanical properties of the utilized materials and the significant impact of the welding process on the mechanical properties of some aluminum alloys. The following subsections discuss the key aspects that are involved in predicting the ultimate strength of welded aluminum stiffened panels.

2.1 MECHANICAL PROPERTIES ACROSS THE HAZ

The mechanical properties across the heat affected zone have a significant influence on the behavior of welded aluminum structures. After the welding process, the area in the vicinity of the welds can be divided into three zones: the weld zone (WZ), heat affected zone (HAZ), and the base metal (BM). The *Aluminum Design Manual* (AA 2020) defines the HAZ to extend 25 mm (1-in) from the centerline of the groove weld or the heel of a fillet weld. Several researchers investigated the change in the mechanical properties within the HAZ (e.g., Nazemi & Ghrib, 2019; Collette, 2022; Hakem et al., 2019; Du et al., 2022). Typical Vickers microhardness (ASTM, 2017) profiles reported in literature (e.g., Hernandez et al., 2013; Pérez et al., 2016; Ilman et al., 2020) show that the WZ and HAZ have lower hardness compared to that of the BM. Figure 2.1 shows a typical hardness profile for a butt weld joint completed with gas metal arc welding (GMAW) as reported in Pérez et al., (2016). These lower hardness values have been shown to correlate with low yield and ultimate tensile strengths for the relevant zones (Lakshminarayanan et al., 2009, Du et al., 2022).

Documents
Document Sharing Hub
Full document details: Strength of Welded Aluminum in Tension

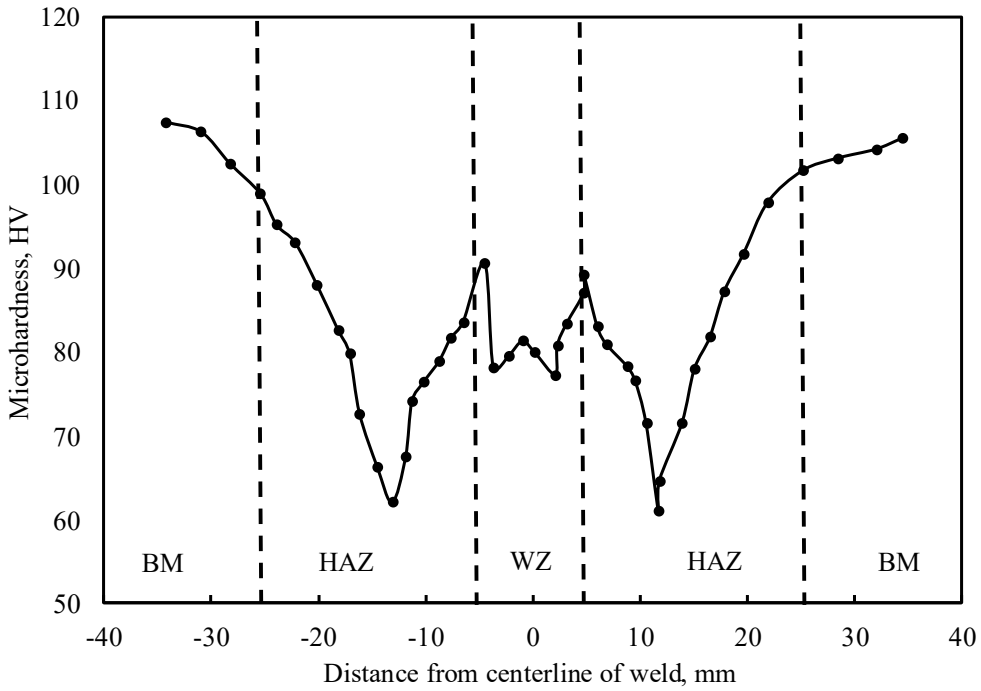


Figure 2.1: Typical hardness profile of butt welded joint (adapted from Pérez et al. (2016)).

The composition of aluminum alloys plays an important role in shaping their strength characteristics. This composition also leads to the deterioration in mechanical properties after welding. Magnesium and silicon, commonly used as alloying elements, react together forming a strengthening precipitate, Mg_2Si. This strengthening precipitate is dispersed homogeneously across the aluminum matrix (Lakshminarayanan et al., 2009) leading to an increase in the yield and ultimate tensile strengths. The welding process affects this strengthening precipitate leading to a change in the mechanical properties (Lakshminarayanan et al., 2009). In general, heat-treated and non-heat-treated alloys require a different choice of welding filler metal. Heat-treated alloys (e.g., 6xxx-series) use filler metals with a different chemical composition than their own to avoid hot cracking along the weld lines; especially at the HAZ (Arun & Ramachandran, 2015). Non-heat-treated alloys (e.g., 5xxx-series) can use a filler alloy that contains the same chemical compositions as the BM. A good example is the 4xxx-series filler alloys that have silicon added to reduce the melting point leading to more fluidity in the molten state (Arun & Ramachandran, 2015). However, for some 6xxx-series alloys, the additional silicon introduced from the filler metal during the welding process lowers the quantity of the Mg_2Si precipitate in the WZ and HAZ compared to the BM region. This goes to the fact that there is not enough magnesium available to react with this surplus amount of silicon to create the strengthening precipitate. As a result, the

Documents
Document Sharing Hub
Full document details: Strength of Welded Aluminum in Tension

mechanical properties in the WZ and HAZ deteriorate after fusion welding (Lakshminarayanan et al., 2009). When silicon becomes excessive in aluminum alloys, chances of intergranular corrosion increase which explains why the 6xxx series alloys are slightly less corrosion resistant than 5xxx series alloys (Davis, 2001).

Another reason that causes the decrease in strength and hardness across the HAZ is the existence of porosity after welding. Several studies have investigated the effect of porosity on the mechanical properties of welded aluminum connections. Liu et al. (2012) investigated the mechanical properties of AA5083 butt welds after being welded using gas tungsten arc welding (GTAW) and GMAW. Scanning electron microscopy (SEM) of both weldments showed the presence of considerable porosity in the GMAW weldment and no porosity in the GTAW weldment. Porosity can be attributed to the presence of hydrogen which is highly soluble in molten aluminum but is of low solubility in the solid state (Poolperm et al., 2020). Hydrogen can be sourced from the base metal, filler metal, and/or shielding gas. Huang et al. (2019) studied the metallurgical and mechanical properties of AA5083 GMAW groove welds for different plate thicknesses and concluded that increasing the plate thickness will in turn increase the porosity in the welded joints. Increasing the thickness will lead to more weld passes and faster solidification rates that may increase the porosity (Bakar et al., 2012).

Heat input also plays a critical role in determining the grain size within the HAZ and, in turn, the extent of deterioration in the mechanical properties. Welding processes such as GTAW and GMAW vary with respect to their heat input levels. GMAW generates more heat because direct current is used and its filler metal is always connected to the positive polarity; however, the GTAW uses alternating current and, thus, the heat input at one end of the electrode is maximum and minimum on the other end (Lakshminarayanan et al., 2009; Arun & Ramachandran, 2015). Accordingly, constant high heat generation is observed with GMAW, while varying heat generation is observed with GTAW. The constant heat generated with GMAW slows down the cooling rate because peak temperatures of the molten weld pool will be reached more frequently. Unfortunately, this creates a fusion zone with wide dendritic spacing leading to inferior mechanical properties (Lakshminarayanan et al., 2009). On the other hand, the heat generated during the GTAW is not as high; this results in a higher cooling rate creating narrower dendritic spacing in the fusion zone (Cruz et al., 2010). This zone possesses better mechanical properties as compared

Documents
Document Sharing Hub
Full document details: Strength of Welded Aluminum in Tension

to those found in the same region in the GMAW weldments (Lakshminarayanan et al., 2009). Bakar et al. (2012) studied the effect of double-sided welds on the microstructure of AA6061 GMAW welded plates. They concluded that the heat from the second pass, alongside the not fully dissipated heat of the first weld pass, altered the cooling rate and resulted in dissolving of the grain boundaries and the drop in the hardness values in those regions.

Although several researchers investigated the change of the mechanical properties across the HAZ, it is still challenging to characterize the stress-strain behavior at different locations across the HAZ. In literature, several studies correlate the change in the hardness across the HAZ to a corresponding change in the yield and ultimate strengths (e.g., Ilman et al., 2020; Pérez et al., 2016). However, such correlation is subjected to significant uncertainty and may not lead to the proper stress-strain profile of the studied region (Collette, 2022). Other researchers used the sectioning approach to characterize the change in mechanical properties across the HAZ (Wang et al. 2006). In this approach, thin coupons are extracted from the HAZ and subjected to tensile testing resulting in more accurate representation of the load-deformation behavior of different regions within the HAZ. More recent studies implemented digital image correlation (DIC) with virtual force method (VFM) to establish such characterization (Nazemi and Ghrib, 2019). In this report, characterizing the stress-strain profiles of different regions within the HAZ is established by extracting coupons from a welded specimens combining the two utilized alloys.

2.2 RESIDUAL STRESSES AND THEIR DISTRIBUTION IN WELDED ALUMINUM JOINTS

Residual stresses and distortion arise from the welding process of aluminum alloys. These stresses may affect the behavior of the welded aluminum component. Residual stresses are stresses that remain in the structural component after welding or fabrication. These stresses would be in the state of global force equilibrium as they are not caused by external loads. Most manufacturing processes result in the development of these stresses due to volume changes that accompany phase transformations, different cooling rates within the same component, and the differential plastic flow characteristics (Nazemi, 2015). The difference in cooling rate within the elements of the same component is the main contributor to the development of residual stresses during and after the welding process (Rossini et al., 2012). Typically, the external surfaces will cool at a faster rate compared to the heated part in the center of the section/plate. As the center of the heated region

Documents
Document Sharing Hub
Full document details: Strength of Welded Aluminum in Tension

starts to cool down, its contraction will be constrained by the cooler external surfaces leading to the development of compressive residual stresses on the external surfaces and tensile stresses at the center. Another factor that can lead to the development of these residual stresses is the localized non-uniform heating during the welding process which is related to the type of welding process and the skill of the welder (James, 2011).

Residual stresses can impact the structural integrity of welded panels subjected to tensile loads (Poolperm et al., 2020). The development of tensile residual stresses in welded connections increase the probability of crack initiation at the weld toe leading to a lower fatigue resistance (Fricke, 2005). Tensile residual stresses can also lead to stress concentration cracking that can be found in the weld ripples and at the start/stop position along longitudinal welds (Mutombo & Du, 2011). Compressive residual stresses, on the other hand, can reduce the propagation rate of cracks leading to a potential positive effect on the fatigue life of the component (Fricke, 2005; Rossini et al., 2012). The overall impact of residual stresses on the fatigue life of a component depends on the geometry, size of the structure, welding technique, material properties, and residual stress distribution.

Several studies in literature focused on quantifying the magnitude of residual stresses due to welding and their distribution. Zhang et al. (2009) concluded that the magnitude of residual stresses in the longitudinal direction of GTAW butt welds is higher than the magnitude in the transverse direction. Further from the weld line, the compressive residual stresses will need to balance out the tensile residual stresses located near the welding region. These tensile residual stresses in the longitudinal direction may reach the yield strength of the base metal in some cases. However, the residual stresses in the transverse direction depend on the welding procedure and the clamping condition of the plates at the far ends parallel to the weld. If it is free, then only compressive residual stresses will be induced due to the Poisson's effect supplementing the restrained longitudinal contraction. If it is clamped mechanically, which is the typical case, the compressive residual stresses induced from the Poisson's effect will get superimposed with some tensile stresses in the transverse direction (McClung, 2007). Figure 2.2 demonstrates the typical distribution of longitudinal and transverse residual stresses in a butt welded joint. Hosseinabadi and Khedmati (2021) compiled and summarized the welding imperfections and extent of the HAZ in their review study on the ultimate strength of welded aluminum structural elements. Following

Documents
Document Sharing Hub
Full document details: Strength of Welded Aluminum in Tension

a similar format, Table 2.1 and Table 2.2 compile existing information from literature regarding the magnitude and distribution of residual stresses in AA5083-H116 and AA6061-T6, respectively. Note that this research utilized T6511 temper; however, the mechanical properties of this temper are expected to be very similar to those of the T6 (ASTM B221).

Based on these tables, it is apparent that several studies reported a tensile residual stress due to welding of 67% of the yield stress of the base metal for AA5083. Some of these studies reported values for the compressive residual stresses outside the HAZ while others simply indicated that they balance out the tensile residual stresses. On the other hand, variability can be seen in the reported tensile residual stresses for the AA6061-T6 due to the different types of welds used (i.e., butt welds, fillet welds).

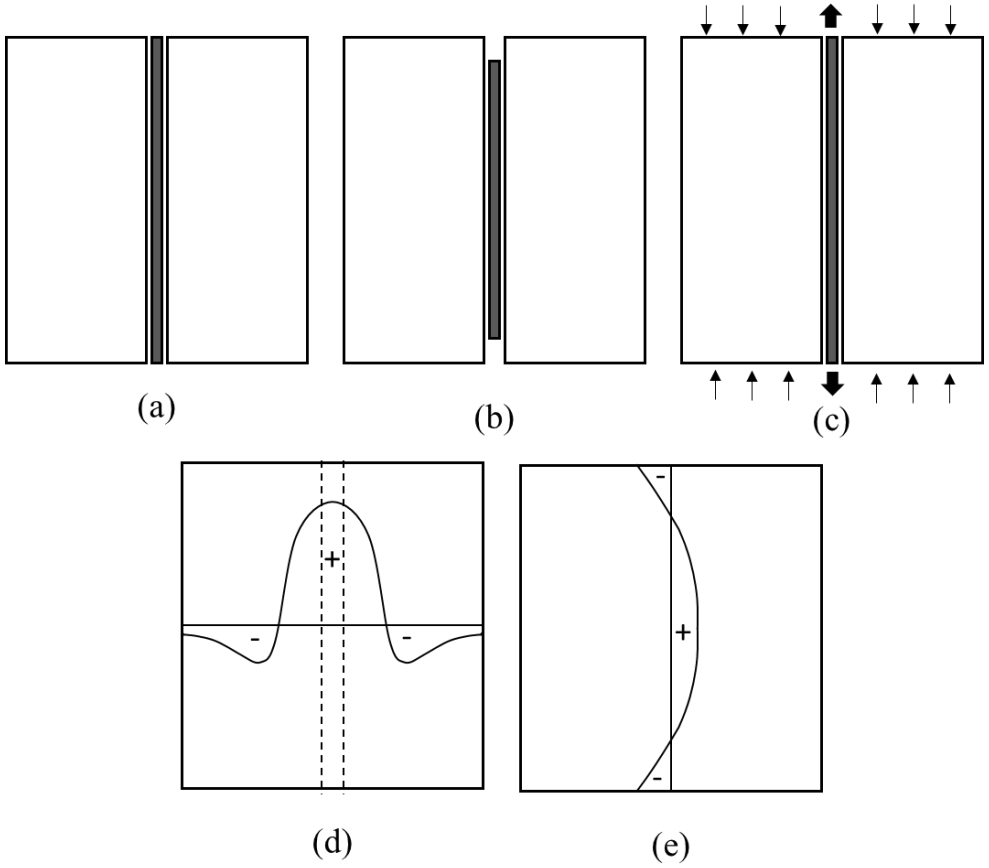


Figure 2.2: Illustrative figure showing the residual stress distribution from butt welds (a) deposition of butt weld, (b) contraction of butt weld, (c) restraint forces between BM and weld, (d) formation of longitudinal residual stresses, and (e) formation of transverse residual stresses (Gurney, 1979).

Documents
Document Sharing Hub
Full document details: Strength of Welded Aluminum in Tension

Table 2.1: Magnitude and distribution of residual stresses in AA5083-H116 reported in literature

Reference	Type of weld	Welding Residual Stress		Residual Stress Distribution	HAZ	
		Tensile, RTS[1]	Compressive, RCS[2]		HAZ extent	$F_{y\,HAZ}$
Zha and Moan (2001)	T Fillet Welds	$F_{y\,RTS} = F_{y\,HAZ}$	In equilibrium with forces arising from tensile residual stresses	• Plate: Rectangular distribution with tension in HAZ and compression in BM • Stiffener: Rectangular distribution with tension at weld tip and compression or tension based on tendon force	25 mmm for 5xxx series; 12.5 mm for 6xxx series (better to be determined by hardness test)	$F_{y\,HAZ} = 0.67\ F_{y\,BM}$
Paik et al. (2005)	Metal Inert Gas (MIG) T Fillet Welds (8mm thick plate with 120 mm stiffener height)	$F_{y\,HAZ} = 0.67\ F_{y\,BM}$ (plate and stiffener)	$F_{y\,HAZ} = -0.12\ F_{y\,BM}$ (plate) $F_{y\,HAZ} = -0.08\ F_{y\,BM}$ (stiffener)	• Plate: Rectangular distribution with tension in HAZ and compression in between stiffeners • Stiffener: Rectangular distribution with tension in welded tip and compression on free end	22.87 mm for plate 13.06 mm for stiffener	$F_{y\,HAZ} = 0.67\ F_{y\,BM}$
Paik et al. (2008)	MIG T Fillet Welds	$F_{y\,RTS} = F_{y\,HAZ}$	$\frac{Fy\ RCS}{Fy\ BM}$ = - 0.161 average for plate $\frac{Fy\ RCS}{Fy\ BM}$ = - 0.137 average for stiffener	Similar to Paik et al. (2005)	23.1mm (average)	$\frac{Fy\ HAZ}{Fy\ BM}$ = 0.777 (average)
Benson et al. (2013)	No experiment conducted	F_y RTS=0.95 $F_{y\,HAZ}$	In equilibrium with tensile residual stresses	• Plate: Rectangular distribution with tension in HAZ and compression in free end	25 mm	$F_{y\,HAZ} = 0.67\ F_{y\,BM}$
Farajkhah and Liu (2016b)	Model was verified by tested data in (Masubuchi ,1980)	• Plate F_y RTS= (0.72-0.77) $F_{y\,BM}$ • Stiffener F_y RTS= (0.82-0.87) $F_{y\,BM}$	• Plate F_y RCS= (-0.18- to -0.36) $F_{y\,BM}$ • Stiffener F_y RCS= (-0.024- to -0.07) $F_{y\,BM}$	• Plate: Rectangular distribution with tension in HAZ and compression in free ends • Stiffener: Rectangular distribution with tension in welded tip and compression on free end	18 to 28 mm from weld line for 5 and 6 mm thick plates 14 mm from weld line for 8 mm thick plate	$F_{y\,HAZ} = 0.67\ F_{y\,BM}$

[1]RTS= Residual Tensile Stresses
[2]RCS= Residual Compressive Stresses

Documents
Document Sharing Hub
Full document details: Strength of Welded Aluminum in Tension

Table 2.2: Magnitude and distribution of residual stresses in AA6061-T6 reported in literature

Reference	Type of weld	Welding Residual Stress		Residual Stress Distribution	HAZ	
		Tensile, RTS[1]	Compressive, RCS[2]		HAZ extent (mm)	$F_{y\,HAZ}$
Yi et al. (2015)	Double Pulse-MIG Fillet welds	Max of 175 MPa (25.4 ksi) in HAZ (5mm away from weld centerline)	Max of -60 MPa (-8.7 ksi) (20 mm away from weld centerline)	• Tensile in HAZ with the curve down. • Compressive stresses balance out tensile stresses. • Stresses were taken from the plate only.	Not reported	Not reported
Yi et al. (2019)	Double Pulse-MIG Butt welds	Max of 190 MPa (27.5 ksi) in HAZ (5mm away from weld centerline)	Max of -60 MPa (-8.7 ksi) (35mm away from weld centerline)	• Tensile in HAZ with the curve down. • Compressive stresses balance out tensile stresses. • Stresses were taken from the plate only.	Not reported	Not reported
Farajkhah et al. (2017)	MIG Butt Welds	• Max of 263 MPa (38.2 ksi) in HAZ (21mm away from weld centerline) • 9 mm thickness	• Range of -30 to -39 MPa (-4.35 to -5.65 ksi) (these balance out the tensile residual stresses) • 9 mm thickness	• The tensile residual stress zone had a width of 80 mm (40 mm from the centerline) • Increasing plate thickness, increased residual stresses (4-, 6-, and 9-mm thickness were tested)	• 15mm from weld line for 4- and 6-mm thick plates • 21mm from weld line for 9 mm thick plate	$F_{y\,HAZ}$ = 0.60 $F_{y\,BM}$
Yi and Park (2022)	GMAW Fillet Welds	• 112.5 MPa (16.3 ksi) in HAZ (10 mm away from weld centerline) • 10 mm thickness	• -12.2 MPa (-1.8 ksi) (80 mm away from weld centerline) • 100 mm thickness	• Tensile in HAZ with curve down. • Compressive stresses balances out tensile stresses • Stresses were taken from plate only	Not reported	$F_{y\,HAZ}$ = 0.63 $F_{y\,BM}$
Zhao et al. (2021)	MIG Butt Welds	• 89.9 MPa (13 ksi) in HAZ (15mm away from weld centerline) • 10.5 mm thickness	• -88.9 MPa (-12.9 ksi) (90 mm away from weld centerline) • 10.5 mm thickness	• Tensile in HAZ with curve down. • Compressive stresses balances out tensile stresses	11.4	Not reported

[1]RTS= Residual Tensile Stresses
[2]RCS= Residual Compressive Stresses

Documents
Document Sharing Hub
Full document details: Strength of Welded Aluminum in Tension

2.3 VARIABILITY IN THE MECHANICAL PROPERTIES OF ALUMINUM ALLOYS

The literature review conducted as part of this work highlighted the presence of high variability in the reported mechanical properties of aluminum alloys. A main parameter that significantly impacts the mechanical properties is the chemical composition of the aluminum alloy. Tercelj et al. (2013) investigated the effect of the chemical composition on the mechanical properties of AA6082. The study concluded that a small increase in the alloying elements can have a major impact on the mechanical properties. For instance, a 33% increase in manganese leads to 5% increase in the elongation. However, copper has an opposite effect on the elongation. The same study also shows that the relationship between the mechanical property of interest (e.g., the yield stress) and the content of alloying elements is far more complex than just a linear proportionality with the content of a single alloying element. In addition to the chemical composition, material production parameters such as the extrusion ratio and ram speed affect the mechanical properties. Material elongation increased with the increase in the extrusion ratio and decrease in the ram speed. The yield stress, however, increased with increasing the ram speed (Tercelj et al., 2013).

Heat treatment is another factor that impacts the mechanical properties of aluminum alloys, specifically, the duration and temperature the alloy is subjected to during the precipitation hardening process play an important role (Siddiqui et al., 2000; Ozturk et al., 2010). Other studies in literature highlighted the impact of the specimen attributes and test procedure on the obtained mechanical properties. These include the coupon dimensions and thickness, rolling direction, and strain rate. Børvik et al. (2009) conducted tensile tests on specimens with four different thicknesses (i.e., 15, 20, 25, and 30 mm) made from A5083-H116 to investigate the effect of the thickness on the mechanical properties. The tests reported a yield stress of 278, 230, 152, and 224 MPa (40.3, 33.5, 22, and 32.5 ksi) for the 15, 20, 25, and 30 mm, respectively. This variation was attributed to the different manufacturing mechanisms that can be used to obtain the H116 temper with a particular thickness. Najib et al. (2015) tested the effect of rolling direction on the mechanical properties of AA5083. An increase in the ultimate strength as the angle increases from 0^o to 90^o was observed, while a decrease in the Young's Modulus was noticed.

The strain rate was also shown to affect the load-deformation behavior of aluminum coupons. Tucker et al. (2010) investigated the effect of the strain rate on the material behavior and

Documents
Document Sharing Hub
Full document details: Strength of Welded Aluminum in Tension

the associated failure mechanism of multiple aluminum alloys including AA6061-T6 through a group of tensile, compressive, and torsional tests. The study covered three strain rates: 0.001/s, 1/s, and 1000/s and reported similar values of ultimate tensile strength and elongation at the two lower rates, while an increase in the ultimate tensile strength and elongation (6.7% and 43%, respectively) occurred at the highest strain rate. Ambriz et al. (2013) also investigated the tensile behavior of AA6061-T6 under different strain rates. Quasi-static and dynamic strain rates, equal to 5.25×10^{-4}/s and 1500/s, were applied to tensile coupons. A 5.5% increase in the ultimate tensile strength and 78% increase in elongation were observed with the higher rates, however, a 40% drop in the yield strength was also seen.

As for AA5083-H116, Darras et al. (2013) investigated the load-deformation behavior of AA5083 under strain rates of 0.001/s, 0.01/s, and 0.1/s and concluded that at these strain rates, the ductility and yield strength of this aluminum alloy show very low sensitivity to the strain rate. Other studies in literature suggests that the AA5083-H116 may exhibit a negative strain rate sensitivity at a certain range of strain rates. Clausen et al. (2004) performed tensile tests over four different strain rates: 4×10^{-4}/s, 3.95/s, 122/s, and 1313/s. Normally, increasing the strain rate would lead to an increase in the flow stress; however, the results showed a negative strain rate sensitivity highlighted by a decrease in the flow stress with the increase in the strain rate, as the strain rate increases from 10^{-5}/s to 10/s. After that, a positive strain rate sensitivity was observed. In the case of negative strain rate sensitivity, redistribution of the stresses at the necking zone is prevented due to the softening resulting in fracture to occur in at lower strains. This range of strain rates that can be accompanied by negative strain rate sensitivity is critical since marine vessels can be subjected to strain rates that lie in the10^{-3}/s region (Giannotti & Stambaugh, 1984).

Among the notable efforts targeted to quantify the variability associated with the mechanical properties of aluminum alloys, Skejić et al. (2021) compiled the mechanical properties of several aluminum alloys from 12,542 coupon tests reported in literature. For the AA6061-T6, the paper reported the yield strength to follow Lognormal distribution with a mean of 263 MPa (38.15 ksi) and a 7% coefficient of variation based on 27 samples. Moreover, a Lognormal distribution with a mean of 279 MPa (40.5 ksi) and a 6% coefficient of variation was reported for the ultimate tensile strength of the same alloy. Although the paper reported the mechanical properties of AA5083, it was not of the same temper as the plates utilized in this report (i.e., H116).

Documents
Document Sharing Hub
Full document details: Strength of Welded Aluminum in Tension

Accordingly, more testing and statistical analysis are still needed to establish the probabilistic descriptors of the mechanical properties of various aluminum alloys.

Studies in literature that reported the mechanical properties of the two alloys utilized in this report were collected as part of this literature survey. Table 2.3 and Table 2.4 present the findings associated with each alloy. The mean value of the yield strength of AA5083-H116 obtained from 10 different studies was 220 MPa (32 ksi) with a coefficient of variation of 8.65%, while the mean of the ultimate tensile strength is 325 MPa (47.2 ksi) with a coefficient of variation of 6.7%. The lower bound for the reported ultimate tensile strength of AA5083 is 300 MPa (43.5 ksi) while the upper bound is 353 MPa (51.2 ksi). For the AA6061-T6 alloy, the mean and coefficient of variation of the tensile yield strength based on 9 published studies is 272 MPa (39.5 ksi) and 7%, respectively. The mean value of the reported ultimate strength is 310 MPa (45 ksi) with a coefficient of variation of 6%. The lower bound of the reported ultimate tensile strength is 262 MPa (38 ksi) while the upper bound is reported as 335 MPa (48.6 ksi). Quantifying the uncertainty associated with these parameters is essential in establishing reliability-based design procedures that reflect the realistic behavior of welded aluminum panels. To maximize the safety of designed structures, design specifications, e.g., *Aluminum Design Manual* (AA 2020) and *Eurocode 9 Design of Aluminum Structures* (CEN 2007), utilize a low bound of the mechanical properties. This conservatism may result in an uneconomical design.

Based on this review, it seems that the variability in the mechanical properties of aluminum alloys stems from two main sources. The first is related to the chemical composition and production techniques while the second is related to the test methods and protocols. Regardless of the source, these uncertainties affect our ability to predict the true strength of the components under normal operational conditions and more research is needed to quantify and reduce these uncertainties. Given this high variability, to aid in understanding the behavior of the tested large-scale specimen, it was decided to conduct a parallel ancillary testing program aiming at quantifying the stress-strain behavior of the material utilized for fabricating the specimens.

Documents
Document Sharing Hub
Full document details: Strength of Welded Aluminum in Tension

Table 2.3: Mechanical properties of AA5083-H116.

Reference	**Yield Tensile Strength, F_{ty}** MPa (ksi)	**Ultimate Tensile Strength, F_{tu}** MPa (ksi)
Zha and Moan (2001)	235 (34.075)	349 (50.605)
Romhanji and Popović (2006)	215 (31.175)	305 (44.225)
Collette (2007)	214 (31.03)	300 (43.4)
Paik (2009)	239 (34.655)	353 (51.185)
Cueca et al. (2012)	215 (31.175)	305 (44.225)
Dutra et al. (2015)	220 (31.94)	328 (47.56)
Jesus et al. (2017)	220 (25.375)	300 (43.5)
KumarSingh et al. (2018)	228 (33.06)	317 (45.965)
Huang et al. (2019)	206 (29.87)	305 (44.225)
Ilman et al. (2020)	230 (33.35)	346 (50.126)

Table 2.4: Mechanical properties of AA6061-T6.

Reference	**Yield Tensile Strength, F_{ty}** MPa (ksi)	**Ultimate Tensile Strength, F_{tu}** MPa (ksi)
Collette (2007)	240 (34.8)	262 (38)
Lakshminarayanan et al. (2009)	300 (43.79)	335 (48.43)
Ashwani Kumar et al. (2014)	280 (40.6)	310 (44.95)
Khotiyan and Kumar (2014)	280 (40.6)	310 (44.95)
Arun and Ramachandran (2015)	240 (34.8)	295 (42.63)
He et al. (2016)	280 (40.02)	310 (44.95)
Pérez et al. (2016)	270 (39.3)	322 (46.69)
Ramaswamy et al. (2020)	275 (39.875)	318 (46.11)
Zhang et al. (2020b)	276 (40.02)	322 (46.69)

Documents
Document Sharing Hub
Full document details: Strength of Welded Aluminum in Tension

2.4 TENSILE STRENGTH PREDICTION OF WELDED ALUMINUM PANELS

2.4.1 Aluminum Design Methods

The latest form of the *Aluminum Design Manual* (AA 2020), published by the Aluminum Association, adopts the mechanical properties of the base metal reported in the ASTM of the designated aluminum alloy or in accordance with the guidelines put forth by the AWS D1.2 (2014) for welded aluminum alloys. The length of the HAZ, as defined in AA (2020), extends to 25 mm (1-in) from the centerline of the groove weld or the heel of the fillet weld. In the presence of transverse welds, where the entire cross section is heat affected, the strength of the cross section can be computed by multiplying the tensile ultimate strength of the weld-affected wrought material, F_{tuw} by the effective net area, A_e which corresponds in this case to the HAZ. In the presence of longitudinal welds, the strength of the cross section is computed as the sum of the strength of the unaffected material away from the HAZ and the heat affected material in the HAZ. The nominal tensile strength P_n, can be computed as (AA 2020)

$$P_n = \left((F_{tu} * (A_e - A_{ewz}))/K_t\right) + (F_{tuwz} * A_{ewz}) \quad (1)$$

where F_{tu} is the ultimate tensile strength of unaffected zones, A_e is the effective net area, A_{ewz} is the area of the welded zone, K_t is the tension coefficient (taken as 1 for the aluminum alloys utilized on this report), and F_{tuwz} is the tensile ultimate strength of the weld-affected zone which can be computed using the weighted average approach as (AA 2020)

$$F_{tuwz} = \left((F_{tuwBM} * A_{BM}\right) + (F_{tuwFM} * A_{FM}))/\, A_{wz} \quad (2)$$

$$A_{wz} = A_{BM} + A_{FM}$$

F_{tuwBM} is the tensile ultimate strength of weld-affected base metal given in Table A.4.3 of the *Aluminum Design Manual* (AA 2020), F_{tuwFM} is the tensile ultimate strength of the filler metal given in Table A.4.6 of AA (2020), A_{BM} is the area of the base metal in the weld affected zone, A_{FM} is the area of the filler metal, and A_{wz} is the area of the weld-affected zone that extends 25 mm (1-in) from the heel of the fillet weld. In this report, for the specimen with longitudinal and transverse welds, the entire cross section will be treated as weld-affected in the transverse direction and the specimen is expected to fail in that region.

Documents
Document Sharing Hub
Full document details: Strength of Welded Aluminum in Tension

The European specifications, *Eurocode 9 Design of Aluminum Structures* (CEN 2007), follows a different path for quantifying the design capacity of the HAZ adjacent to fillet welds. It applies a softening factor, $\rho_{u,haz}$, to the HAZ that depends on the alloy, temper, and the welding process (i.e., MIG or Tungsten Inert Gas (TIG)). Furthermore, the width of the HAZ, b_{haz} depends on the welding process and the material thickness. The MIG welding process can be applied to all thicknesses, however, the TIG is used with thickness up to 6 mm. TIG welding on higher thicknesses leads to a larger HAZ and would require a more severe softening factor. The design resistance of the HAZ adjacent to a fillet weld for the tensile forces perpendicular to the failure plane is given in Equation 3. This needs to be checked at the fusion boundary and at the toe of the weld.

$$\sigma_{haz,Ed} \leq \frac{f_{u,haz}}{\gamma_{Mw}} \tag{3}$$

where $\sigma_{haz,Ed}$ is the design normal stress perpendicular to the weld axis, $f_{u,haz}$ is the characteristic strength of the HAZ which relies on the reduction factor discussed before, and the γ_{Mw} is the partial factor for welded joints which 1.25. Similar models are provided for shear forces and combined shear and tensile forces.

Other specifications, such as the *ABS Rules for Building and Classing High-Speed Craft* (ABS 2023) rely on the allowable stress approach for aluminum structural design. The stresses are computed using finite element (FE) analysis and compared against the allowable stress. These allowable stresses are provided as a fraction of the proof stress of the HAZ, the type of structure under consideration, and the type of loading. Proof and ultimate strengths are provided for certain welded aluminum alloys; however, the gauge length is not specified, which makes it difficult to compare these allowable stresses to values reported in other design codes. Unfortunately, the extent of the HAZ is also not explicitly defined. On the other hand, certain weld bend tests and weld qualification procedures are required to ensure that the required ductility of the welds is met.

2.4.2 FE modelling for predicting the tensile strength of welded aluminum panels

Finite element analysis has been utilized in literature to predict the capacity of aluminum components. Dørum et al. (2010) analyzed the failure of welded aluminum connections using solid, shell, and cohesive-zone elements. The solid element model was used as the reference

Documents
Document Sharing Hub
Full document details: Strength of Welded Aluminum in Tension

solution for the other two models; however, its mesh sensitivity and need for a small mesh size to fully capture the strain concentrations increase the modeling effort and computational cost. The shell element model was also found to be mesh sensitive; additionally, strain concentrations occurred at lower load levels when compared to the model with solid elements due to the neglection of the out-of-plane normal stresses. The cohesive-zone model lumped the weakest zone of the HAZ between the solid elements with lengths equal to the surrounding mesh. The results were satisfactory in comparison to the base solid element model especially that this model is mesh insensitive. Unfortunately, no validation with experimental results was conducted.

Sensharma et al. (2011) studied the possibility of modeling the extent and location of the HAZ explicitly in the FE model. The HAZ in their study had its own mechanical properties. Three variants were modelled: all base metal with no HAZ, a single HAZ, and a combination of base metal and HAZ on an aluminum stiffened panel consisting of 3 bays and 4 stiffeners. The results came with all base metal models being unrealistic and all HAZ being too conservative. The analysis was conducted under tensile, compressive, and bending loading. The results from the analysis on the stiffened panel showed an ultimate compressive strength prediction close to the that resulting from the model proposed by Paik et al. (2005). Unfortunately, no comparison to tensile testing results was conducted. The width of the HAZ was assumed to be three times the thickness of the plate; however, this model used shell elements which did not allow modelling of welds. Furthermore, the residual stresses were not included in the analysis. However, the need for considering the HAZ in the FEM was clearly highlighted in their study.

Woelke et al. (2017) studied the effect of modelling undermatched welds, commonly found in ship construction, on the behavior of aluminum welded connections. The study advocates the need to account for undermatched weld properties in the design process since they are associated with a decrease in the strength of the HAZ which generally governs the strength of the connection. Furthermore, the presence of undermatched welds affects the plastic fracture behavior and crack initiation and propagation within the weld metal or the HAZ. In designing large-scale aluminum structures, shell elements with in-plane dimensions greater than the thickness are typically utilized. This may preclude the ability to account for through-thickness deformations that may affect the behavior especially in the presence of undermatched welds. To address this, an approach that includes a calibrated cohesive zone was presented in their study to predict the ductile failure of

Documents
Document Sharing Hub
Full document details: Strength of Welded Aluminum in Tension

aluminum structures with undermatched welds. The results were promising; however, this technique relies on the assumption that plasticity is only localized in the WM and HAZ and that the BM will still be in the elastic domain. Accordingly, it may not be applicable for welded joints with matched welds.

Nazemi and Ghrib (2019) studied the change in mechanical properties across the HAZ in welded aluminum connections. They identified multiple zones within the HAZ each with its own mechanical properties. This can be seen in Figure 2.3 for AA6061-T6. The x-marker in the figure represents the ultimate fracture point. These stress-strain curves were developed from the local strain measurements captured by the DIC technique. Using the DIC, material constitutive models were created using the virtual fields method (Germain, 1986). Furthermore, the results from the material constitutive models were validated using a fully coupled thermal-metallurgical-mechanical simulation. This simulation was divided into three stages. The first included the usage of the standard three-dimensional double ellipsoid heat source model proposed by Goldak et al. (1984) to model the welding on a mesh of 8-node solid elements. The second covered utilizing the metallurgical model proposed by Myhr and Grong (1991) for considering the phase transformations of heat affected aluminum and integrating it into the simulation. The last part is the simulation of a tensile test through the application of a fixed boundary condition at one end and an applied displacement on the opposite end. The finite element results were in good agreement with experimental ones; therefore, the approach was utilized to simulate the behavior of welded plate-column connection.

Farajkhah and Liu (2016a) studied how the fabrication method can affect the ultimate strength of aluminum hull girders. Their study included friction stir welding (FSW), MIG butt welding, and MIG fillet welds. One of the aims of their study was to simulate the three welding procedures and study the welding induced residual stresses, HAZ, and distortions to be used later in quantifying the strength of aluminum hull girders. The simulation of MIG welding was divided into multiple stages. Thermal loads were applied by adopting the birth/death feature in ANSYS (ANSYS, 2015) that mimics the accumulation of the molten metal droplets on the welded specimen. The time-dependent temperature distribution of the welded material was obtained through nonlinear transient thermal analysis. This time dependent temperature distribution was used to represent the increment in the position of the passing weld torch by being added as load

Documents
Document Sharing Hub
Full document details: Strength of Welded Aluminum in Tension

steps. After all the welding sequences were finished, the specimen cooling to room temperatures was also simulated resulting in obtaining the welding induced residual stresses and distortions. To allow for possible separation and/or sliding between the stiffener and plate before the deposition of welding, spring elements were defined in the interface region. Temperature and residual stresses profiles were validated against experimental test results conducted by Masubuchi (1980). The paper reported that the width of the HAZ around the weld line for MIG butt and MIG fillet welds was 30 mm (1.18-in) and 40 mm (1.57-in), respectively. The paper showed that this approach of FEM can simulate the MIG welding process. However, this modeling approach is complex and may not be suitable for large-scale structures.

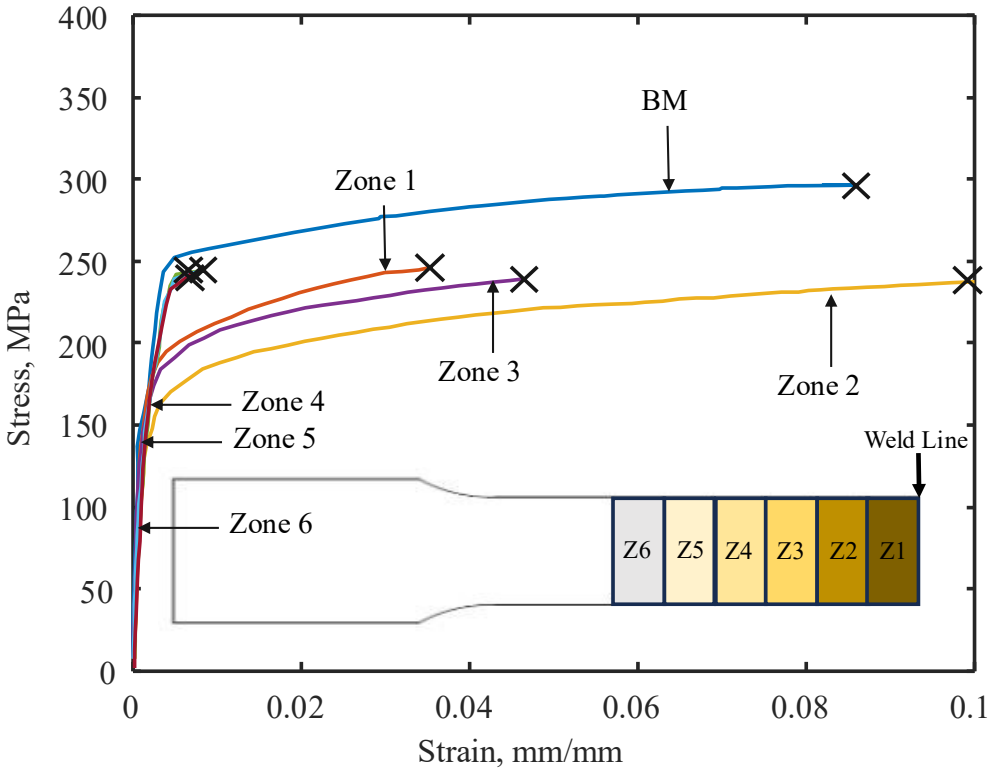


Figure 2.3: Stress-Strain curves for the HAZ of AA6061-T6 (adapted from Nazemi and Ghrib (2019)).

Collette (2022) investigated, experimentally and numerically, the strength of plates with transverse, non-load carrying fillet welds. The finite element model utilized different mechanical properties across the HAZ and included the fillet weld and definition of the residual stresses. Heating was applied to the model then specimen cooling was considered until it reached room temperature. This caused residual stresses to build up at the HAZ and BM within the model. The

Documents
Document Sharing Hub
Full document details: Strength of Welded Aluminum in Tension

mechanical properties across the HAZ were correlated to hardness test data and incorporated into the model through parallel sectioning of the material. The HAZ was divided into four zones with each section given the corresponding mechanical properties. Eighteen large scale specimens with transversely welded stiffeners were experimentally tested to cover two fillet weld sizes (i.e., 5 mm and 8 mm) and continuous versus intermittent fillet welds. The author recommended the use of more regions for the sectioned HAZ to fully capture the change in mechanical properties across the HAZ. It was also noted that correlation between the mechanical properties and hardness test data may be subjected to high variability. Nevertheless, the study showed that localized failures will happen in the HAZ and start at the toe of the weld when using non-load carrying fillet welded connections. In addition, the study highlighted the need for further investigations into the tensile capacity of welded aluminum components since they have a significant influence on the overall behavior of the structure.

Based on this literature survey, it is apparent that several knowledge gaps need to be addressed for the proper quantification of the tensile behavior of welded aluminum components. One of the main gaps is the lack of large-scale experimental data that covers the tensile behavior of aluminum components with different welding configurations. The presence of such experimental data would assist in the proper understanding of the behavior of ship hulls and validating the design approaches. A thorough experimental testing program that quantifies the impact of welding parameters on the behavior of large-scale welded aluminum would also assist in identifying the key factors associated with the reduction of strength/ductility due to welding. Furthermore, additional numerical analysis is necessary to assess the best practices for proper modelling of the welds, HAZ, and residual stresses especially when incorporated in large complex structures. Comprehensive assessment of the variability in the mechanical properties of aluminum alloys coupled with detailed reliability analysis would reflect on optimized design codes that provide safe yet economic designs. This report addresses some of these gaps by presenting the results of a comprehensive experimental program conducted to quantify the tensile behavior of unstiffened and stiffened large-scale aluminum specimens. The stiffened specimens include transversely stiffened components, longitudinally stiffened components, and the combination of both stiffener types in one specimen. In addition, it discusses a detailed finite element approach capable of capturing the actual behavior of these specimens under tensile loading.

Documents
Document Sharing Hub
Full document details: Strength of Welded Aluminum in Tension

3 EXPERIMENTAL TESTING PROGRAM

Experimental testing was conducted to understand the impact of welded stiffeners on the tensile strength of aluminum panels. The investigation included experimental analysis on large-scale specimens to quantify the effect of stiffeners and investigate the efficacy of different modeling strategies. This testing program included 12 specimens covering flat plates, longitudinally stiffened plates, transversally stiffened plates, and plates with both stiffener types. To properly characterize the material behavior and aid in numerical modeling, ancillary testing was conducted on tensile coupons extracted from the base metal and HAZ. The large-scale specimens and fabricated plates utilized for extracting the tensile coupons were fabricated by AUSTAL USA. The large-scale testing was conducted at the Bert Cooper Engineering Laboratory while the ancillary testing was performed in Endeavor Lab, both located in the Stillwater campus of Oklahoma State University. The following subsections present the details of both testing programs.

3.1 ANCILLARY TESTING

As indicated above, the analysis herein covers two types of aluminum alloys commonly used in ship construction, the AA5083-H116 and AA6061-T6511. Each of the tempers of the used aluminum alloys represent a unique process that yields certain mechanical characteristics. For example, the H in the H116 temper represent the work hardened temper type in which strength is elevated through work hardening. Heat treatment thereafter is optional. Specifically, the H116 temper is applied to 5xxx series alloys with a magnesium content higher than 4% and certain corrosion resistance and mechanical properties are required. On the other hand, the T in the T6 temper represent the heat-treated temper type where heat treatment is used to provide strength for the alloy and may or may not be followed by strain hardening. Specifically, the T6511 temper is heat treated and then artificially aged until the precipitation hardening of the alloy has evolved; next, the extrusion is given a permanent set and straightened to meet required construction tolerances. Coupon tests were needed to properly understand the behavior of the large-scale samples and obtain the mechanical properties to be utilized on the numerical analysis. Furthermore, characterizing the change in the mechanical properties across the HAZ for both aluminum alloys would aid in identifying the variables that govern the behavior of welded stiffened panels. To establish these goals, samples from the base metal plates and welded plates that are fabricated using the same electrode and welding technique utilized for the fabrication of

Documents
Document Sharing Hub
Full document details: Strength of Welded Aluminum in Tension

the large-scale specimens were requested from the fabricator. Figure 3.1 shows the details of the welded specimen requested from the fabricator. Tensile coupon specimens were extracted later from this specimen and used to characterize the behavior of the HAZ and BM.

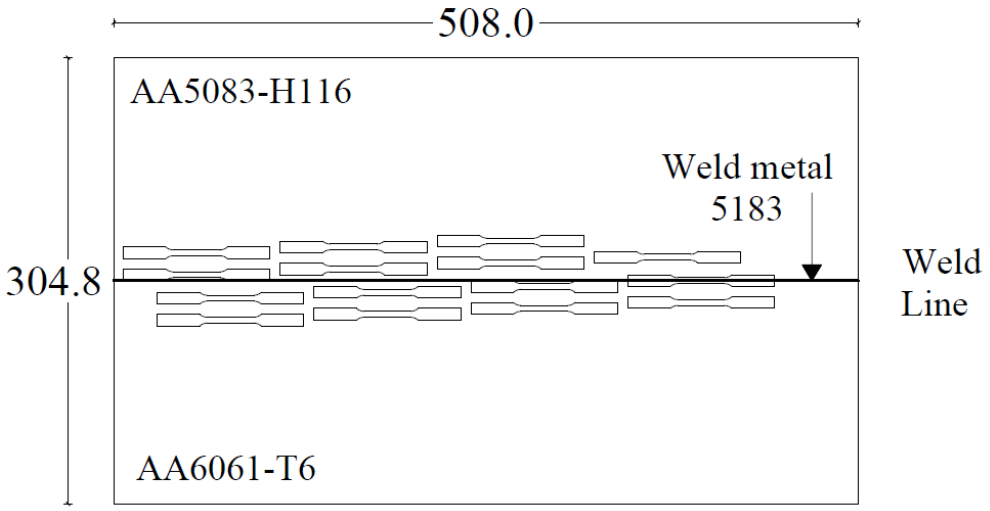


Figure 3.1: Dimensions of welded specimen for coupon testing in millimeters.

The groove welded specimen shown in Figure 3.1, is composed of AA5083-H116 and AA6061-T6511 flat plates that were welded using 5183 filler metal. GMAW welding, with 1.2 mm (3/64-in) diameter ER5183 filler metal, was utilized for constructing all specimens in this test program. The welding was completed under constant voltage (CV) and direct current electrode positive (DCEP) with an amperage range of 185 and voltage of 24.5. The weld travel speed was set at 457 mm/minute (18 inch/minute) and the wire feed speed was 11.43 meters/minute (450 inch/minute). Each plate has dimensions of 508×152×12.5 mm (20×6×0.5-in). A single specimen was created from this welding process. Although the large-scale aluminum specimens, as will be discussed later, utilized plates with a thickness of 8 mm (5/16-in), in lieu of the 12.5 mm (0.5-in) thickness of these plates, it was still believed that this specimen can provide baseline information on the mechanical properties of the HAZ and BM. Tensile coupons with dimensions following ASTM B557 (2023) were extracted from this specimen using a water jet cutting. Figure 3.2 shows the detailed dimensions of these coupons. As shown in Figure 3.1, The coupons were staggered to provide ample space to prevent specimen damage and to allow extracting coupons at different locations within the HAZ. The coupons were extracted at 4, 8, 12, 16, 19, 23, and 27 mm from the center line of the weld for each aluminum alloy. Moreover, a single coupon was cut at the centerline of the weld metal to represent the mechanical properties of the 5183 weld metal. This

Documents
Document Sharing Hub
Full document details: Strength of Welded Aluminum in Tension

would enable evaluating the mechanical properties across the HAZ for the AA5083-H116, AA6061-T6511 and for the 5183 filler metal.

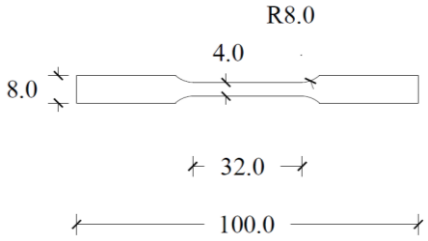


Figure 3.2: Dimensions of coupons that are to be cut using a waterjet in millimeters.

3.2 LARGE SCALE EXPERIMENTAL SETUP

3.2.1 Original Test Setup

The layout of the large-scale aluminum specimens was heavily influenced by the configuration and limitations of the test equipment. Initially, it was intended to utilize a 1,500 KN Instron Universal Testing Machine, shown in Figure 3.3 and available in Bert Cooper lab, for the large-scale specimens. The specimen was designed with an ultimate strength that falls within the capacity of the testing frame following the dimensions of the grip zone of the machine. Figure 3.4 shows the different components of the original test setup. Connection brackets or stiffeners were added between the end plate and test plate to prevent premature failure away from the gauge length.

Documents
Document Sharing Hub
Full document details: Strength of Welded Aluminum in Tension



Figure 3.3: The 1,500 KN Universal Testing Machine.

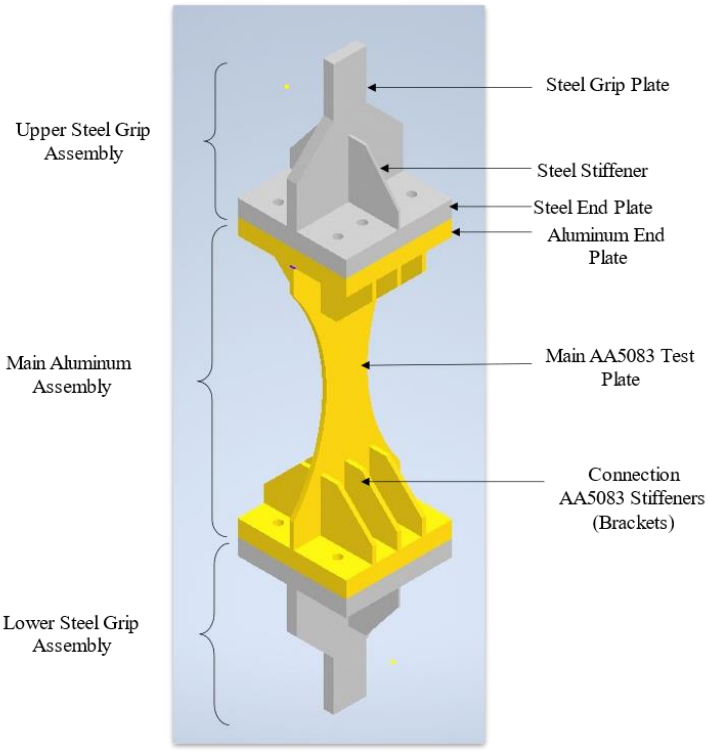


Figure 3.4: 3D render of the original test setup showing various specimen components.

Documents
Document Sharing Hub
Full document details: Strength of Welded Aluminum in Tension

The setup was designed such that the entire assembly would be inserted into the hydraulic grips of the machine with the steel grip assembly connected to the aluminum specimen using steel bolts and square washers on the aluminum side. Figure 3.5 shows the assembly inside the grips of the universal testing machine.

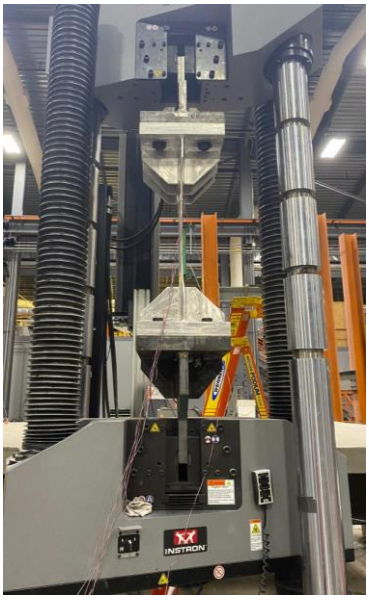


Figure 3.5: Original test setup with assembly in place.

3.2.1.1 Upper and Lower Steel Grip Assemblies

The upper and lower grip assemblies are mainly composed of a grip plate to be inserted into the hydraulic grip slots of the test machine and an end plate that is connected to the aluminum test specimen. Figure 3.6 shows a 3D view of the grip assembly, while Figure 3.7 shows the detailed dimensions of the assembly.

Documents
Document Sharing Hub
Full document details: Strength of Welded Aluminum in Tension

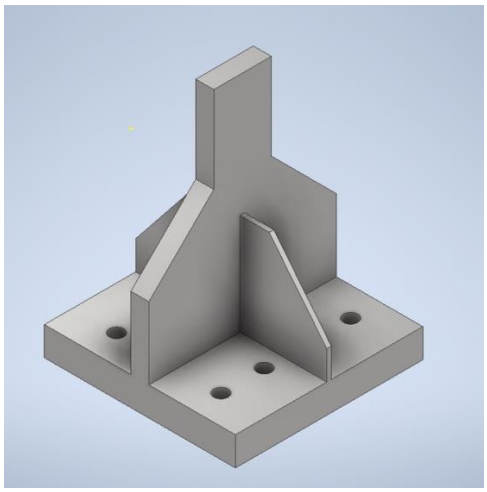


Figure 3.6: 3D render for the Steel Grip Assembly.

The material used for the steel grip assemblies is ASTM A572 Gr. 50 (ASTM A572, 2021). This steel has an ultimate and yield strengths of 449 MPa (65 ksi) and 345 MPa (50 ksi), respectively. This steel grip plate was checked against tensile yield. The steel end plate was designed to resist the bending stresses that would arise during the test using the models in *ANSI/AISC 360* (2016) and Swanson (2003). An 8 mm steel stiffener was added to reduce the stresses on the steel end plate and increase its stiffness. The steel grip plate and the steel end plate were welded using complete joint penetration groove weld based on Table 3.1 of AWS D1.1 (AWS, 2020) with an E70 electrode.

Unfortunately, this setup was eventually not utilized due to testing software malfunctions that occurred while testing the first specimen. Such malfunctions were feared to compromise the integrity experimental results. Therefore, an updated test setup was designed and constructed to complete the experimental testing and ensure the integrity of the results. The new setup utilized the same specimen design with changes applied only to the grip assemblies as will be discussed below.

Documents
Document Sharing Hub
Full document details: Strength of Welded Aluminum in Tension